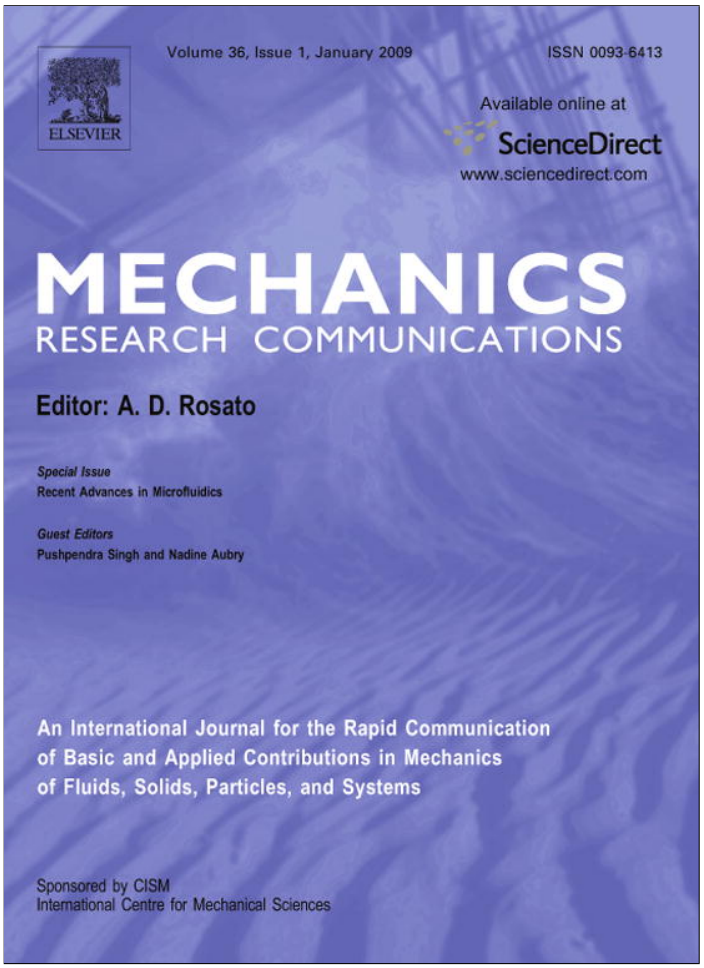

Mechanics Research Communications 36 (2009) 2–9

Contents lists available at ScienceDirect

Mechanics Research Communications

journal homepage: www.elsevier.com/locate/mechrescom

More about the electromechanics of electrowetting

T.B. Jones *

Department of Electrical and Computer Engineering, 304 Hopeman Engineering Building, University of Rochester, Rochester, NY 14627, USA

ARTICLE INFO

Article history:
Received 20 June 2008
Received in revised form 12 August 2008
Available online 18 September 2008

Keywords:
Electromechanics
Electrowetting
Contact angle
Surface tension

ABSTRACT

Classical lumped parameter electromechanics successfully models most observable phenomenology of droplet-based electrowetting and liquid dielectrophoresis. The key to this unifying approach is to express capacitance in terms of the proper mechanical variable. While this capability is easily revealed in modeling microfluidic schemes, where the electrical force drives center-of-mass motions of the liquid, lumped parameter electromechanics also can be adapted for devices such as the liquid lens, where a liquid mass is made to change its shape and is characterized by observable changes in the apparent, liquid/solid contact angle. Because capacitance is usually insensitive to contact angle, irregularities of the liquid configuration, and fringing fields, electromechanical modeling is easy to use. For the case of liquids of finite electrical conductivity, a capacitive- and resistive-based model can be used to predict frequency-dependent effects.

1. Introduction

Droplet-based microfluidic schemes exploiting the electrowetting (EWOD = electrowetting-on-dielectric) and liquid dielectrophoretic (DEP) force mechanisms show promise in many applications. Nowadays, increasingly complex electrode structures for such systems are contemplated, so the need to develop efficient, predictive models for their performance is growing. The prevalent way to calculate the electrical force acting on a droplet in an EWOD device is to treat the effect as an enhancement of the surface force resulting from the voltage-induced change in the contact angle. But there are problems with this approach. First of all, contact angle modulation is not the "prime mover" responsible for center-of-mass droplet motion. It is, in fact, more accurate to regard (i) changes in the contact angle and (ii) center-of-mass motions as distinct observables, both induced by the distributed electrostatic force acting on the free surface of the liquid. In the localized region just above the contact line, the fringing field induces free electric charge upon the surface of the conductive liquid and then exerts a net force on these charges. Second, the contact angle approach grows unwieldy as geometries become more complex. On the other hand, the electromechanical model, based on variable capacitance, is usually easy to implement and offers some opportunity for effective, reduced-order modeling. Even for very complex geometries, advantage may be taken of capacitance calculation tools built into modern finite element computational software to determine the electrical force. Third, in any microfluidic device where the intention is to exploit frequency as an independent control variable, the contact angle model fails completely because of difficulties obtaining a useable relationship between contact angle, frequency, and liquid conductivity.

The objective of this work is to extend the electromechanical interpretation of electrowetting (Jones, 2005) to more practical electrode geometries, such as EWOD droplet transport structures. The lumped parameter, capacitive model is robust and easy to use. In addition, the model is quite amenable to predicting the frequency-dependent behavior of simple, yet

* Tel.: +1 585 275 5233.
E-mail address: jones@ece.rochester.edu

0093-6413/$ - see front matter © 2008 Elsevier Ltd. All rights reserved.
doi:10.1016/j.mechrescom.2008.08.012

practical EWOD geometries using an RC circuit model to establish the voltage distribution. Contact angle-based models do not possess such a capability.

2. The sessile droplet

By far, the most familiar demonstration of electrowetting is the change in shape of a sessile, conducting liquid droplet resting on a dielectric-coated plane electrode when voltage is applied between the droplet and the electrode, see Fig. 1. The strong, localized, electrostatic force acting upon the free surface of the droplet above the contact line causes it to spread, thus increasing its area coverage of the electrode. It is of course convenient to quantify the phenomenon in terms of the observable, voltage-dependent decrease of the apparent liquid/solid contact angle $\theta(v)$. Unfortunately, this point of view has evolved into the questionable physical interpretation that the spreading is due to the change in the contact angle, rather than merely a parallel consequence of the electrostatic force acting near the contact line. The electromechanical analysis summarized below reveals that a capacitive model correctly predicts the change in shape of the droplet and does so without making any direct reference to contact angle.

For convenience, we assume the droplet is small enough so that its surface retains the shape of a spherical cap. The validity of this approximation is established by the dimensionless Bond number *Bo*, which compares the capillary and gravitational forces.

$$Bo = \rho_L g h^2/\gamma_{LV} \tag{1}$$

where h is the height of cap, γ_{LV} is liquid/vapor surface energy per unit area, ρ_L is liquid density, and $g = 9.81\ \mathrm{m/s^2}$. If $Bo \ll 1$, capillarity overwhelms gravity and the free surface of the droplet is essentially spherical. Folding in the constraint that the droplet has fixed volume V yields a convenient set of relationships between height h, radius of the contact a, radius of the spherical cap r, and contact angle θ, as defined in Fig. 1 (Berthier, 2008).

$$h^3 + 3a^2h - 6V/\pi = 0 \tag{2a}$$

$$r = (h^2 + a^2)/2h \tag{2b}$$

$$\cos(\theta) = \sqrt{1 - (a/r)^2} \tag{2c}$$

Appendix A shows that Eq. (2a), cubic in h, has a single real root. While any of the geometrical quantities defined in Fig. 1 for the spherical cap geometry might be designated as the mechanical state variable for a virtual work-based, electromechanical formulation, the radius of the circular contact, a, is probably the best choice because it identifies physically reasonable capillary and electrostatic forces per unit length of contact line.

A useful, preliminary exercise is to consider the hydrostatics of the droplet in the absence of the electrical force, that is, $v = 0$. The spherical surface area and the contact area of the sessile droplet, A_{LV} and A_{LS}, respectively, are

$$A_{LV}(a) = 2\pi r(a)h(a) \text{ and } A_{LS}(a) = \pi a^2 \tag{3}$$

Then, the total surface energy of the system is

$$W_\gamma(a) = \gamma_{LV}A_{LV} + \gamma_{LS}A_{LS} + \gamma_{SV}(A_E - A_{LS}) \tag{4}$$

where subscripts LV, LS, and SV refer, respectively, to the liquid/vapor, liquid/solid, and solid/vapor interfaces, and A_E represents the constant, total area of the dielectric-coated plane electrode. As already suggested, choice of a as the mechanical variable, while arbitrary, allows direct computation of an effective interfacial force per unit length of contact line f^γ.

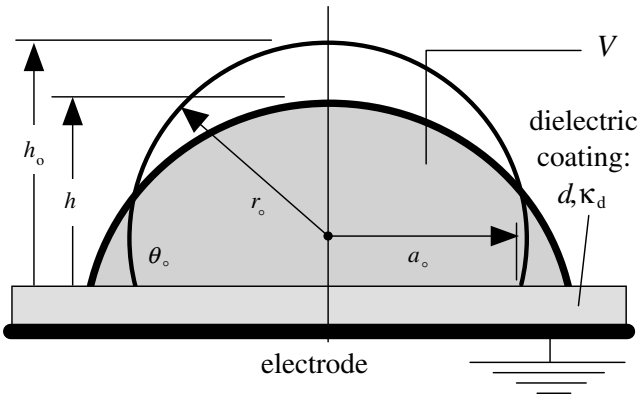

Fig. 1. Side view of a sessile droplet resting on the dielectrically coated electrode with h, r, a, and θ defined. The droplet, which is conducting, acts as the deformable electrode of a capacitor, subject to the constraints of constant volume and a spherical cap shape. Variables identified by the subscript "o" represent values when voltage $v = 0$.

$$f^{\gamma}(a) = \frac{-1}{2\pi a}\frac{\partial W_{\gamma}}{\partial a} \tag{5}$$

Using Eq. (4) and the definitions of the geometrical factors in this equation, we obtain

$$f^{\gamma}(a) = \gamma_{SV} - \gamma_{LS} - \gamma_{LV}\cos\theta \tag{6}$$

The familiar Young equation (see de Gennes et al., 2004), relating the equilibrium contact angle θ_c to the surface energies of the three interfaces, results from imposing the equilibrium condition, $f^{\gamma} = 0$.

$$\gamma_{LV}\cos\theta_c + \gamma_{LS} - \gamma_{SV} = 0 \tag{7}$$

Note that, while the above derivation is based on the approximation that the sessile droplet has the shape of a spherical cap, Eq. (7) is in fact far more general. Refer to Henriksson and Eriksson (2004) for more about meniscus shape.

3. Electromechanics of droplet deformation

In response to the electrostatic force, the droplet changes shape and spreads. We conceptualize the lumped parameter electromechanical model with the conservative system shown in Fig. 2. Together, the conducting droplet and the dielectrically-coated plane electrode supporting it form capacitance C, which can be expressed in terms of droplet contact area $A_{LS} = \pi a^2$. In most practical electrowetting applications, the dielectric coating is very thin, $d \ll a$, justifying neglect of fringing fields. Thus,

$$C(a) \approx \frac{\kappa_d \varepsilon_o A_{LS}}{d} = \frac{\kappa_d \varepsilon_o \pi a^2}{d} \tag{8}$$

Eq. (8) is actually correct for any cylindrically symmetric shape assumed by the droplet, and thus the generality of Eq. (7) is extended. If $a \sim d$, the fringing fields at the contact line can no longer be ignored, and a correction factor is needed (Plonsey and Collin, 1961).

$$C_{\text{corrected}}(a) \approx \frac{\kappa_d \varepsilon_o}{d}[\pi a^2 + 2ad\ln(2\pi a/d)] \tag{9}$$

Imposing the energy conservation condition on the coupling shown in Fig. 2 gives

$$dWe = \upsilon dq - 2\pi a f^{e} da \tag{10}$$

where $q = C(a)\upsilon$ is the electric charge and $We(q,a)$ is the electrical energy storage of the coupling. The electrical force per unit length of contact line, f^e, is interpreted as acting radially outward and parallel to the plane electrode at the contact line.

In EWOD devices, voltage υ rather than charge q is constrained, so it becomes convenient to change state variables from (q,a) to (v,a) using a Legendre transform. Following Woodson and Melcher (1968), we define a type of free energy called the coenergy $We'(v,a)$.

$$We + We' = vq \tag{11}$$

Using Eq. (11) in Eq. (10) gives

$$dWe' = q d\upsilon + 2\pi a f^{e} da \tag{12}$$

Invoking a crucial, defining condition on the force of electrical origin, that is, $f^e(v = 0, a) = 0$, Eq. (12) may be integrated in (v,a) space to obtain an expression for $We'(v,a)$. The familiar result is

$$We'(\upsilon, a) = \frac{1}{2}C(a)\upsilon^2 \tag{13}$$

The analytical nature of this function means that

$$f^{e} = \frac{1}{2\pi a}\left.\frac{\partial We'}{\partial a}\right|_{\upsilon=\text{constant}} = \frac{1}{2\pi a}\frac{\upsilon^2}{2}\frac{dC}{da} \tag{14}$$

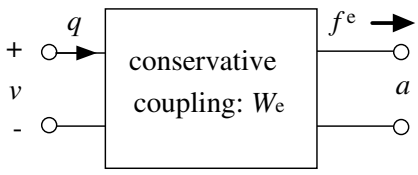

Fig. 2. The conservative electromechanical coupling, with electrical and mechanical ports on the left and right, respectively, is used to evaluate the distributed force of electrical origin f^e acting radially around the edge of the droplet and causing it to spread.

The force of electrical origin per unit length of contact line is thus determined by the dependence of the system capacitance upon the mechanical variable a.

$$f^{e} = \frac{\kappa_d \varepsilon_o}{2d} \upsilon^2 \tag{15}$$

It is crucial to recognize that this force, while directly attributable to the distributed electrical forces near the contact line, has been determined here with no reference to the fringing field. In fact, the capacitance expression used, Eq. (8), explicitly ignores fringing. To gain some perspective about this apparent paradox, it is only necessary to refer to classical thermodynamics, another energy-based discipline, which for example successfully predicts most of the important temperature, pressure, and volume related behavior of gases without detailed knowledge of gas kinetics. Berge's original analysis (Berge, 1993) is also based on an energy argument and likewise avoids the need to know the details of the fringing field.

4. Electromechanical equilibrium of sessile droplet

For the electrically stressed droplet to be in equilibrium, $f^{e} + f^{\gamma} = 0$. After some algebraic manipulation, this equilibrium reduces to

$$\cos\theta(\upsilon) = \cos\theta_c + \frac{\kappa_d \varepsilon_o \upsilon^2}{2d\gamma_{LV}} \tag{16}$$

which is Berge's equation for voltage-dependent, apparent contact angle on a dielectric-coated electrode (Berge, 1993). Alternatively, one may define a potential energy function, $U(v,a) \equiv W_{\gamma}(a) - We'(v,a)$, in which case Eq. (16) results from setting $\partial U/\partial a = 0$.

Obtaining Eq. (16) directly from minimizing a potential energy function teaches us that the electromechanical approach is fully consistent with previously published analyses of the capillary behavior of sessile droplets. It is important to reiterate that the above derivation of the force of electrical origin f^{e} requires no knowledge of either the contact angle of the droplet or its hydrostatic profile. Furthermore, a force calculation based on the Maxwell stress tensor, which likewise may be performed without knowing any details of the liquid profile close to the dielectric-coated electrode, yields exactly the same result (Jones, 2002,).

5. Electrowetting with two coplanar electrodes

Consider a pair of very thin, coplanar electrodes of identical width w, separated by a uniform gap g and coated with a dielectric layer of thickness d and dielectric constant κ_d. Atop the structure and straddling these electrodes is a conducting liquid droplet, see Fig. 3. For present purposes, this droplet is assumed to be two-dimensional, i.e., uniform across the electrode width w, though this approximation is voided in the next section. Voltage υ is applied between the two electrodes. The droplet is electrically floating; capacitive voltage division determines its electrostatic potential. To determine the x-directed force acting on the droplet using lumped parameter electromechanics, the only requirement is the system capacitance. Again neglecting fringing fields, the capacitances per unit width on the left and right sides of the droplet are, respectively,

$$C_1(x) = \kappa_d \varepsilon_o (L - x)/d \text{ and } C_2(x) = \kappa_d \varepsilon_o (L + x)/d \tag{17}$$

Because the droplet is not grounded, the net capacitance is the series combination of C_1 and C_2.

$$C(x) = \frac{C_1 C_2}{C_1 + C_2} = \frac{\kappa_d \varepsilon_o}{2Ld}(L^2 - x^2) \tag{18}$$

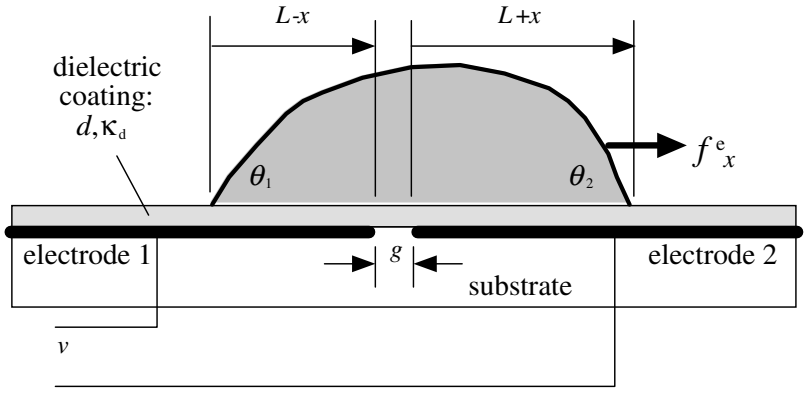

Fig. 3. Side view of basic coplanar electrode geometry of width w relevant to electrowetting-based microfluidic conductive droplet actuation and transport. Initially, the droplet is assumed to be two-dimensional, but this simplification is readily eliminated, as explained in the analysis accompanying Fig. 4.

We use coenergy per unit width, $We' = C(x)v^2/2$, to calculate the force of electrical origin.

$$f_x^e = \left.\frac{\partial We'}{\partial x}\right|_{v=\text{constant}} = \frac{v^2}{2}\frac{dC}{dx} = -\frac{\kappa_d \varepsilon_o v^2}{2Ld}x \tag{19}$$

Eq. (19) is readily checked against the commonly employed contact angle-based approach, the starting point being the force per unit length of contact line from Berge's equation, from Berthier (2008, p. 174),

$$f_x^{EW} = \frac{\kappa_d \varepsilon_o v_{layer}^2}{2d} \tag{20}$$

Capacitive voltage division determines the voltage drops across the layers on the left and right sides.

$$v_1 = \frac{C_2}{C_1 + C_2}v = \frac{L + x}{2L}v \text{ and } v_2 = \frac{C_1}{C_1 + C_2}v = \frac{L - x}{2L}v \tag{21}$$

The total electrical force is the vector sum of the terms on the left and right sides.

$$f_x^{EW} = -\frac{\kappa_d \varepsilon_o v_1^2}{2d} + \frac{\kappa_d \varepsilon_o v_2^2}{2d} \tag{22}$$

Using the expressions for v_1 and v_2 from Eq. (21) in Eq. (22) reproduces Eq. (19), the result already obtained using lumped parameter electromechanics.

Note that lumped parameter electromechanical analysis avoids the need to deal with details of the quantitative distribution of voltage between the two sides, as well as the liquid profile close to the contact line or the fringing field. In the next section, it is shown that the capacitive modeling approach is sufficiently robust to handle a droplet of arbitrary profile.

6. Three-dimensional droplets

The droplets in an electrowetting-based droplet transport structure seldom if ever conform to the 2D model employed above. Instead, they have a sometimes slightly irregular but generally rectangular outline with rounded corners as illustrated in Fig. 4. To calculate the force acting on the droplet using Eq. (20) directly would seem to require knowledge of this profile; however, Berthier (2008) has shown that the total force exerted on the portion of a droplet covering an electrode depends only on the electrode width w and is independent of shape. This result is easily re-confirmed using the capacitive/electromechanical approach. Fig. 4 shows the top view of an irregular droplet, which straddles the two electrodes just like the one in Fig. 3. It is evident that, if the shape remains fixed during translational motion along the structure in the x direction, the derivatives of capacitance, dC_1/dx and dC_2/dx, are independent of position, equal in magnitude, and opposite in sign.

$$\frac{dC_1}{dx} = -\frac{dC_2}{dx} = -\kappa_d \varepsilon_o / d \tag{23}$$

The two contributions to the electromechanical force may now be computed.

$$f_x^e = \frac{v_1^2}{2}\frac{dC_1}{dx} + \frac{v_2^2}{2}\frac{dC_2}{dx} \tag{24}$$

Substituting the expressions for v_1 and v_2 from Eq. (21) into Eq. (24) yields Eq. (19), the result obtained using the simpler 2D assumption, thus showing that droplet outline has no influence on the net electromechanical force.

7. Frequency-dependent droplet electromechanics

The biggest advantage for the electromechanical modeling approach to droplet-based EWOD accrues for variable frequency AC voltage excitation. It is by now well-established that the electrical force exerted on semi-conductive liquids, such

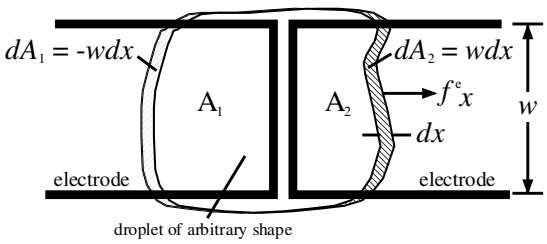

Fig. 4. Top view showing outline of a conducting liquid droplet bridging two coplanar electrodes of identical width w. Even if the droplet profile is irregular, as long as its shape remains fixed as it moves in the x direction, then $dA_1 = -dA_2$ and $dC_1/dx = -dC_2/dx$. With the constant shape constraint, the net force is independent of the droplet outline.

as DI water, many biological media, ethylene glycol, as well as some alcohols, having electrical conductivities $\sigma \sim 10^{-5}$ to 10^{-1} S/m, exhibit strong frequency dependence (Jones et al., 2003, 2004, 2005). This dependence manifests itself over virtually the entire practical range of driving voltage frequencies: $\sim 10^2$ Hz to ~ 1 MHz. Behavior at low frequency corresponds to electrowetting (EWOD) and at high frequency to liquid dielectrophoresis (DEP). Here, a modeling approach based on contact angle, Eq. (22), or any sort of generalization of Berge's equation, Eq. (16), must falter because of the great difficulty of obtaining a simple, frequency-dependent predictive relationship for the apparent contact angle. This difficulty stems inevitably from the finite conductivity of the liquid; for one thing, it is virtually impossible to formulate an unambiguous definition for the droplet-to-plane-electrode voltage that accounts for frequency. More particularly, the electric field and thus the electrostatic energy are not longer concentrated in the dielectric layer under the droplet.

The electromechanical method circumvents such difficulties by using an RC circuit model to determine the distribution of the voltage. Assume the voltage is of the sinusoidal AC form $\upsilon(t) = \mathrm{Re}[\underline{v}e^{j\omega t}]$, where $\underline{v}$ is the phasor voltage, $j = \sqrt{-1}$, ω is radian frequency, and t is time. Further, assume that ω exceeds the frequency of any observable fluid surface disturbances. In this case, we need consider only the time averages of electrical forces. See Fig. 5, which depicts the capacitances and conductances of the circuit model. Note that a planar floating electrode has been added on top to simplify formulation of these circuit quantities. As long as $d \ll D < g$, fringing fields will not be important. Then, the capacitances and conductances per unit width are

$$C_{w1} = \kappa_w \varepsilon_o (L - X)/D, \quad G_{w1} = \sigma_w (L - X)/D, \quad C_{d1} = \kappa_d \varepsilon_o (L - X)/d, \tag{25a}$$

$$C_{w2} = \kappa_w \varepsilon_o (L + X)/D, \quad G_{w2} = \sigma_w (L + X)/D, \quad C_{d2} = \kappa_d \varepsilon_o (L + X)/d, \tag{25b}$$

The distribution of voltage amongst the four capacitive elements is obtained using impedance division. The four phasor voltages $\underline{v}_{w1}$, $\underline{v}_{d1}$, $\underline{v}_{w2}$, and $\underline{v}_{d2}$ across these elements are:

$$\underline{\upsilon}_{w1,d1,w2,d2} = \frac{Z_{w1,d1,w2,d2}}{Z_{w1} + Z_{d1} + Z_{w2} + Z_{d2}} \underline{\upsilon} \tag{26}$$

where

$$Z_{w1} = \frac{D}{(j\omega\kappa_w\varepsilon_o + \sigma_w)(L - x)}, \quad Z_{d1} = \frac{d}{(j\omega\kappa_d\varepsilon_o)(L - x)} \tag{27a}$$

$$Z_{w2} = \frac{D}{(j\omega\kappa_w\varepsilon_o + \sigma_w)(L + x)}, \quad Z_{d2} = \frac{d}{(j\omega\kappa_d\varepsilon_o)(L + x)} \tag{27b}$$

are the complex impedances. The net, time-average force per unit width of the structure, $\langle f_x^e \rangle$, is the sum of four terms, one corresponding to each of the four energy-storing capacitors.

$$\langle f_x^e \rangle = \frac{1}{2}\left[|\underline{\upsilon}_{w1}|^2 \frac{dC_{w1}}{dx} + |\underline{\upsilon}_{d1}|^2 \frac{dC_{d1}}{dx} + |\underline{\upsilon}_{w2}|^2 \frac{dC_{w2}}{dx} + |\underline{\upsilon}_{d2}|^2 \frac{dC_{d2}}{dx} + \right] \tag{28}$$

Combining the previous definitions into Eq. (28), we obtain a frequency-dependent, time-average force per unit width of the electrodes acting on the droplet.

$$\langle f_x^e \rangle = -\frac{\varepsilon_o \upsilon^2}{2}\frac{x}{l}\left[\frac{\kappa_w}{D}\left\{ \frac{\left(\frac{\omega\kappa_d\varepsilon_o}{d}\right)^2}{\left[\omega\varepsilon_o\left(\frac{\kappa_w}{D} + \frac{\kappa_d}{d}\right)\right]^2 + \left(\frac{\sigma_w}{D}\right)^2} \right\} + \frac{\kappa_d}{d}\left\{ \frac{\left(\frac{(\omega\kappa_w\varepsilon_o)}{D}\right)^2 + \left(\frac{\sigma_w}{D}\right)^2}{\left[\omega\varepsilon_o\left(\frac{\kappa_w}{D} + \frac{\kappa_d}{d}\right)\right]^2 + \left(\frac{\sigma_w}{D}\right)^2} \right\} \right] \tag{29}$$

The electromechanical force, linearly dependent on x but independent of the outline of the droplet, is analogous to a mechanical spring, exerting a frequency-dependent, restoring force that attracts the droplet toward stable equilibrium at the midpoint, $x = 0$.

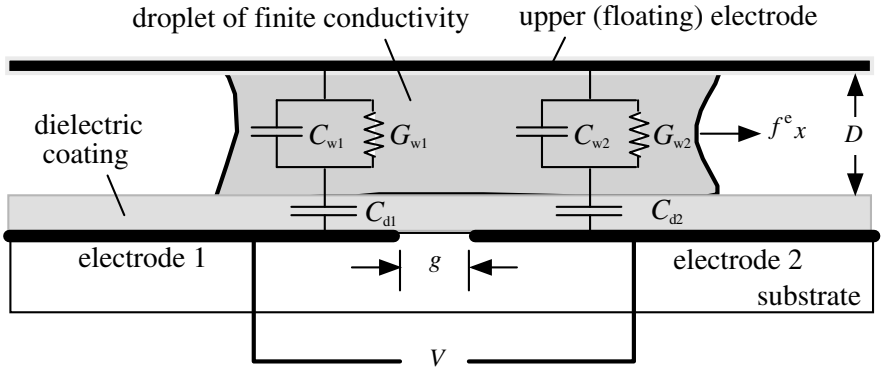

Fig. 5. Side view showing circuit model for electromechanical actuation of semi-conductive liquid droplet. The upper plane electrode is electrically floating and has a very thin dielectric layer that may be ignored in the RC circuit model.

8. Frequency limits of time-average electromechanical force

To provide some physical interpretation for Eq. (29), it is instructive to obtain limiting expressions for the low frequency (EWOD) and high frequency (DEP) values of the force $\langle f_x^e \rangle$.

$$\langle f_x^e \rangle = -\frac{\kappa_d \varepsilon_o \upsilon^2}{2d}\frac{x}{L}, \quad \omega << \sigma_w/\kappa_w\varepsilon_o \tag{30a}$$

$$\langle f_x^e \rangle = -\frac{\varepsilon_o \upsilon^2}{2}\frac{\kappa_d\kappa_w/Dd}{\kappa_d/d + \kappa_w/D}\frac{x}{L}, \quad \omega >> \sigma_w/\kappa_w\varepsilon_o \tag{30b}$$

These limits correspond to conditions where the semiconductive, dielectric liquid behaves effectively like a perfect conductor or a perfect insulator, respectively. As expected, Eq. (30a) is the same as Eq. (19), while Eq. (30b), independent of the liquid conductivity σ, represents purely dielectrophoretic actuation.

9. Conclusion

The electromechanical derivations presented in this paper require no information about contact angle, liquid profile above the contact line, or the fringing field. This is so despite the fact that the EWOD effect is due to the strong, localized fringing field acting on the free surface of the liquid above the contact line. Lumped parameter electromechanics, based on a virtual work approach, inherently does not require such detailed information to treat the observable, translational motions in microfluidic devices. Further, it does not even pinpoint the actual location where the electrical force is acting. There is no need for it to do so. Accuracy and modeling efficiency depend only on having good information about derivatives of the system capacitances and the distribution of voltage, obtainable from the appropriate circuit model. This observation is key to understanding why the capacitive-based method works: net translational displacement of a liquid droplet affects the differential system capacitance, and this capacitance enjoys a linear relationship to energy. In more complex devices, there may arise the need to compute capacitances by numerical means but, once obtained, such data can be folded directly into a lumped parameter analysis, largely preserving the advantage of reduced-order modeling.

A further, compelling advantage of lumped parameter electromechanical treatment of electric-field-coupled, droplet-based microfluidic structures is that it facilitates reduced-order modeling even when the liquid has finite electrical conductivity and when AC voltage excitation is used. The only requirement is an RC circuit model for the microfluidic device that incorporates the dependence upon the correct mechanical variable of all capacitive and resistive elements. It is unlikely that an approach based on contact angle modulation can achieve such generality.

This paper promotes use of lumped parameter electromechanics as a preferred modeling approach for microfluidic devices involving manipulation and translational motion of droplets. Yet, as shown in the analysis of the sessile droplet (Fig. 1), an electromechanical model also can be utilized to predict shape changes of virtually stationary liquid masses as long as their geometry is not too complex. While this statement may be true, one may argue from an entirely utilitarian viewpoint that the contact angle model still suffices as an engineering tool in certain applications such as the liquid lens (Berge and Peseux, 2000).

Acknowledgements

The author has benefited from conversations about electrowetting held over the years with Bruno Berge and Mathieu Maillard (Varioptic, SA), Frieder Mugele (Twente University), Terry Blake (Eastman Kodak Ltd. UK, now retired), and others. Financial support from Eastman Kodak Company, Corning, Inc., the Center for Electronic Imaging Systems (University of Rochester) and the Laboratory for Laser Energetics (University of Rochester) is gratefully acknowledged.

Appendix A

Eq. (2a) for h, the height of the spherical cap, fits the standard canonic form of a reduced cubic equation.

$$h^3 + \alpha h + \beta = 0 \tag{A1}$$

where $\alpha = 3a^2$ and $\beta = -6V/\pi$. Further, it satisfies an inequality, $\beta^2/4 + \alpha^3/27 > 0$, guaranteeing the existence of a single, real, physical root (CRC, 1959). An analytical expression for this root is

$$h(a,V) = \sqrt[3]{\frac{3V}{\pi} + \sqrt{\left(\frac{3V}{\pi}\right)^2 + a^3}} - \sqrt[3]{\sqrt{\left(\frac{3V}{\pi}\right)^2 + a^3} - \frac{3V}{\pi}} \tag{A2}$$

Eq. (A2) may be combined with Eqs. (2b) and (2c) to obtain various useful analytical expressions amongst θ, r, a, h, and V.

References

Berge, B., 1993. Electrocapillarité et mouillage de films isolants par l'eau. CR. Acad. Sci. Paris III 317, 157–163.

Berge, B., Peseux, J., 2000. Variable focal lens controlled by an external voltage: an application of electrowetting. Europ. Phys. J. E – Soft Matter 3, 159–163.
Berthier, J., 2008. Microdrops and Digital Microfluidics. William Andrew, Norwich, NY (USA).
CRC, 1959. Standard mathematical tables, Chemical Rubber Co., Cleveland (USA), p. 358.
De Gennes, P., Brochart-Wyart, F., Quéré, D., 2004. Capillarity and Wetting Phenomena. Springer, New York. p. 17.
Henriksson, U., Eriksson, J.C., 2004. Thermodynamics of capillary rise: why is the meniscus curved. J. Chem. Ed. 81, 150–154.
Jones, T.B., 2002. On the relationship of dielectrophoresis and electrowetting. Langmuir 18, 4437–4443.
Jones, T.B., 2005. An electromechanical interpretation of electrowetting. J. Micromech. Microeng. 15, 1184–1187.
Jones, T.B., Fowler, J.D., Chang, Y.S., Kim, C.-J., 2003. Frequency-based relationship of electrowetting and dielectrophoretic liquid microactuation. Langmuir 19, 7646–7651.
Jones, T.B., Wang, K.L., Yao, D.J., 2004. Frequency-dependent electromechanics of aqueous liquids: electrowetting and dielectrophoresis. Langmuir 20, 2813–2818.
Kang, K.H., 2002. How electrostatic fields change contact angle in electrowetting. Langmuir 18, 10318–10322.
Plonsey, R., Collin, R., 1961. Principles and Applications of Electromagnetic Fields. McGraw-Hill, New York. p. 162.
Wang, K.L., Jones, T.B., 2005. Electrowetting dynamics of microfluidic actuation. Langmuir 21, 4211–4217.
Woodson, H.H., Melcher, J.R., 1968. Electromechanical Dynamics, Part 1. Wiley, New York (Chapter 3).